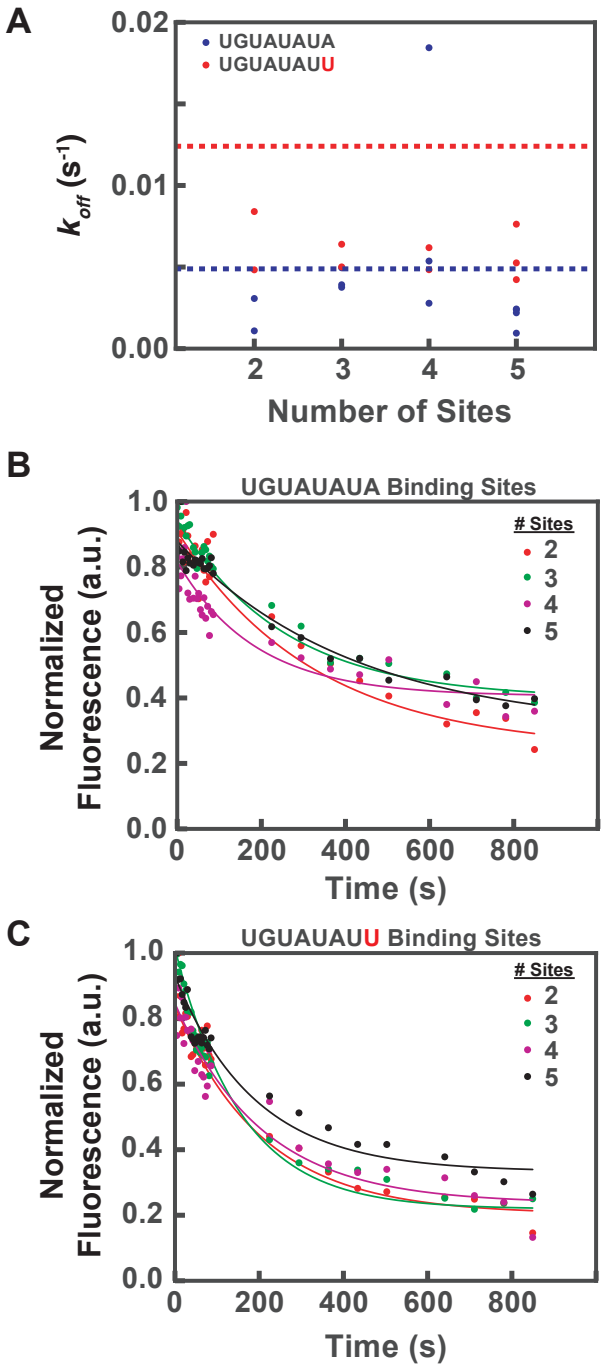

Figure S1: Comparison of protein dissociation from RNAs with different number of protein binding sites. (A) Dissociation rate constants as a function of the number of binding sites. Median dissociation constants for single RNA sites are indicated with dashed lines. (B, C) Fluorescence data and single exponential fits for representative constructs with different numbers of identical UGUAUAUA (B) and UGUAUAUU (C) binding sites.

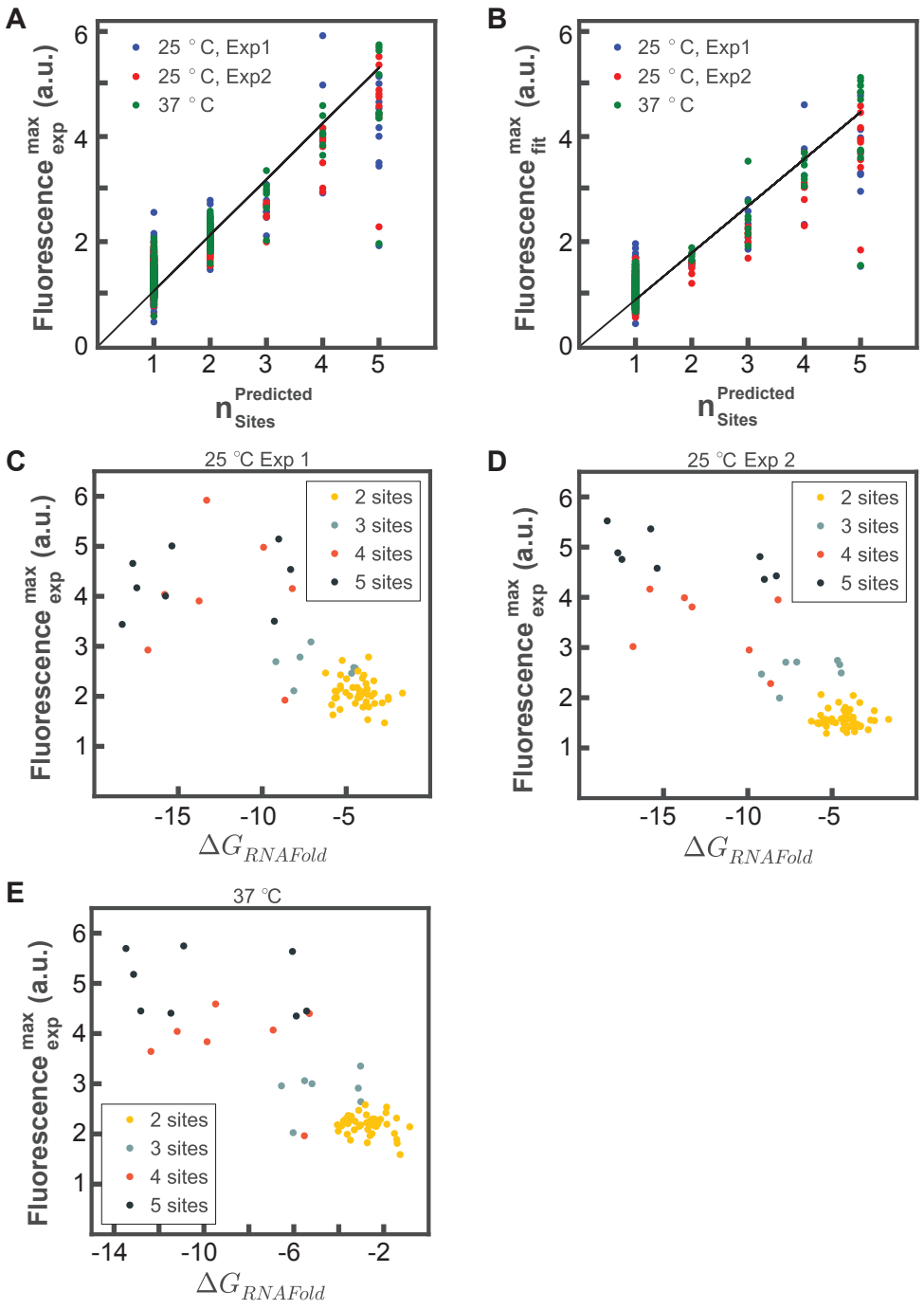

Figure S2: Relationship between maximum fluorescence and number of proteins binding sites. (A) Maximum experimental fluorescence plotted against the number of binding sites. (B) Maximum fit fluorescence plotted against the number of binding sites. (C-E) Maximum experimental fluorescence plotted against the predicted RNA structure for RNAs containing different numbers of PUM2 binding sites for two replicates at 25 °C (C, D) and at 37 °C (E).

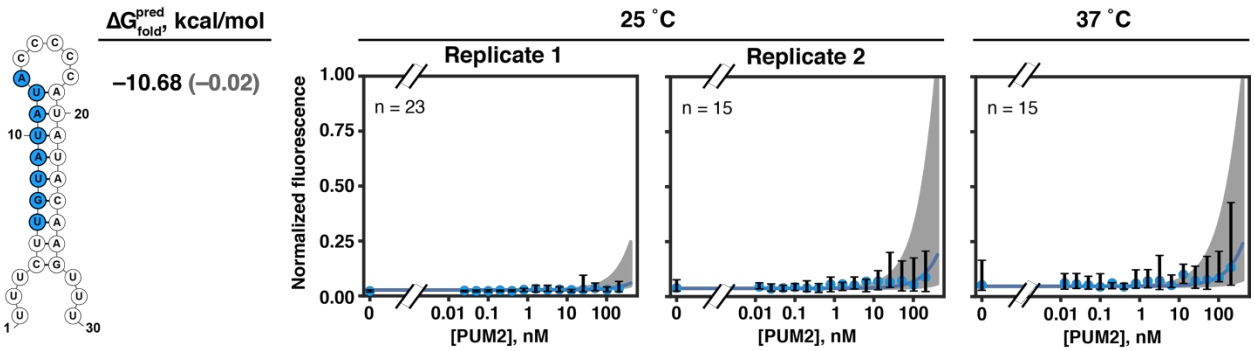

Figure S3: Binding to RNA containing single PUM2 binding sites involved in stable RNA structure at 25 °C and 37 °C (Becker et al. 2019).

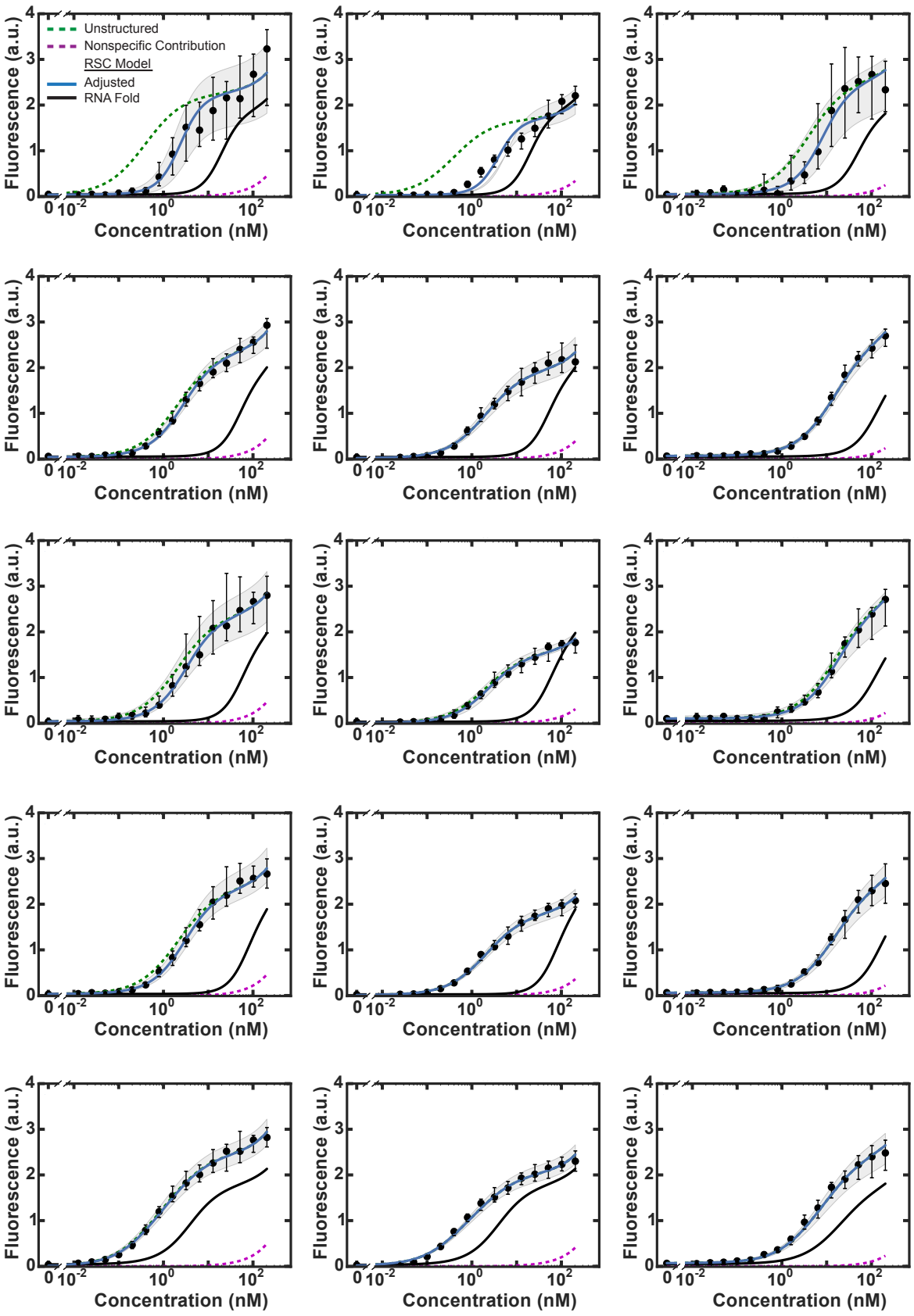
Unstructured
Nonspecific Contribution
RSC Model
Adjusted
RNA Fold
Fluorescence (a.u.)
Concentration (nM)
0
10^{-2}
10^{0}
10^{2}
0
1
2
3
4

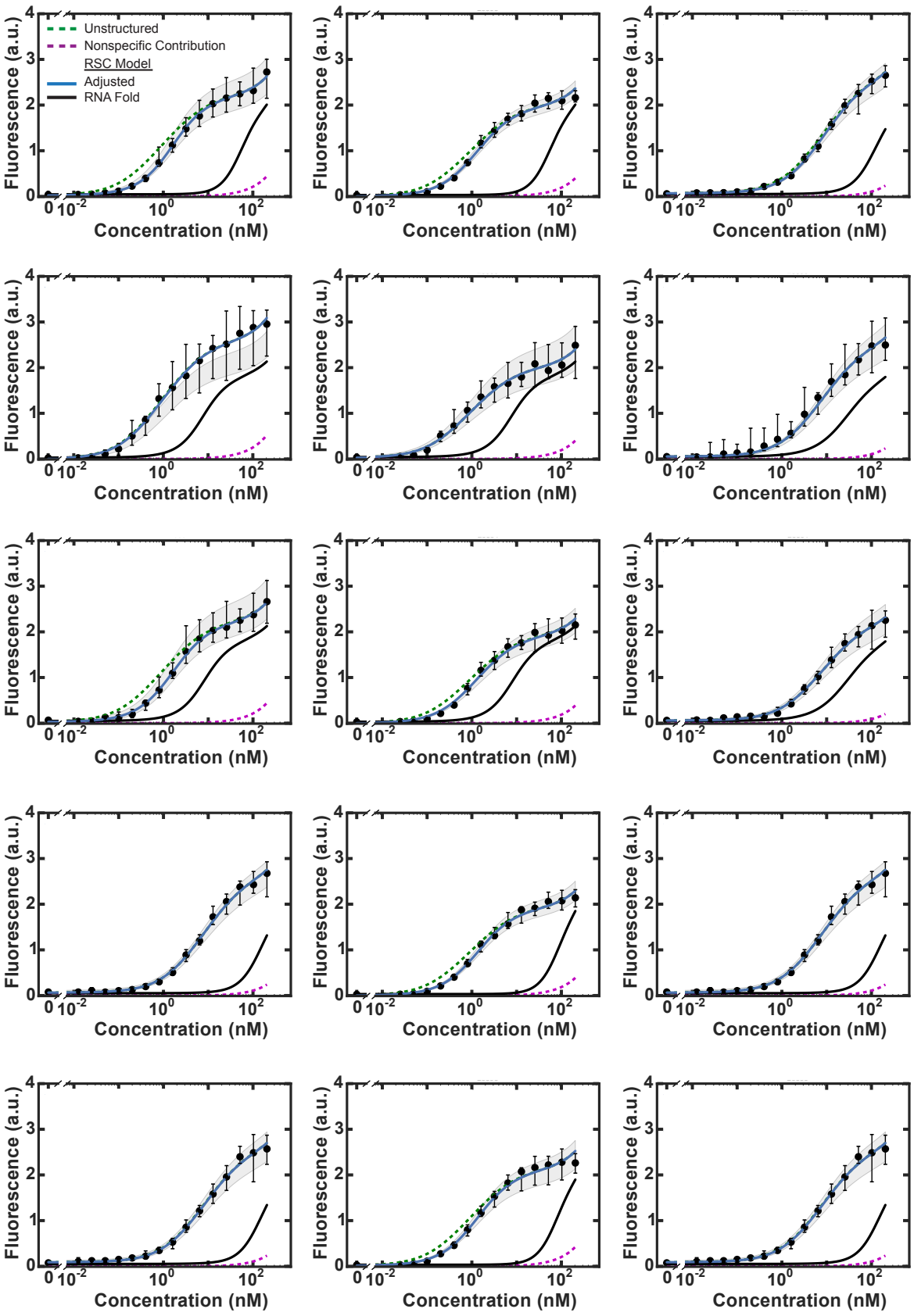
Unstructured
Nonspecific Contribution
RSC Model
Adjusted
RNA Fold
Fluorescence (a.u.)
Concentration (nM)
0
10^{-2}
10^{0}
10^{2}
0
1
2
3
4

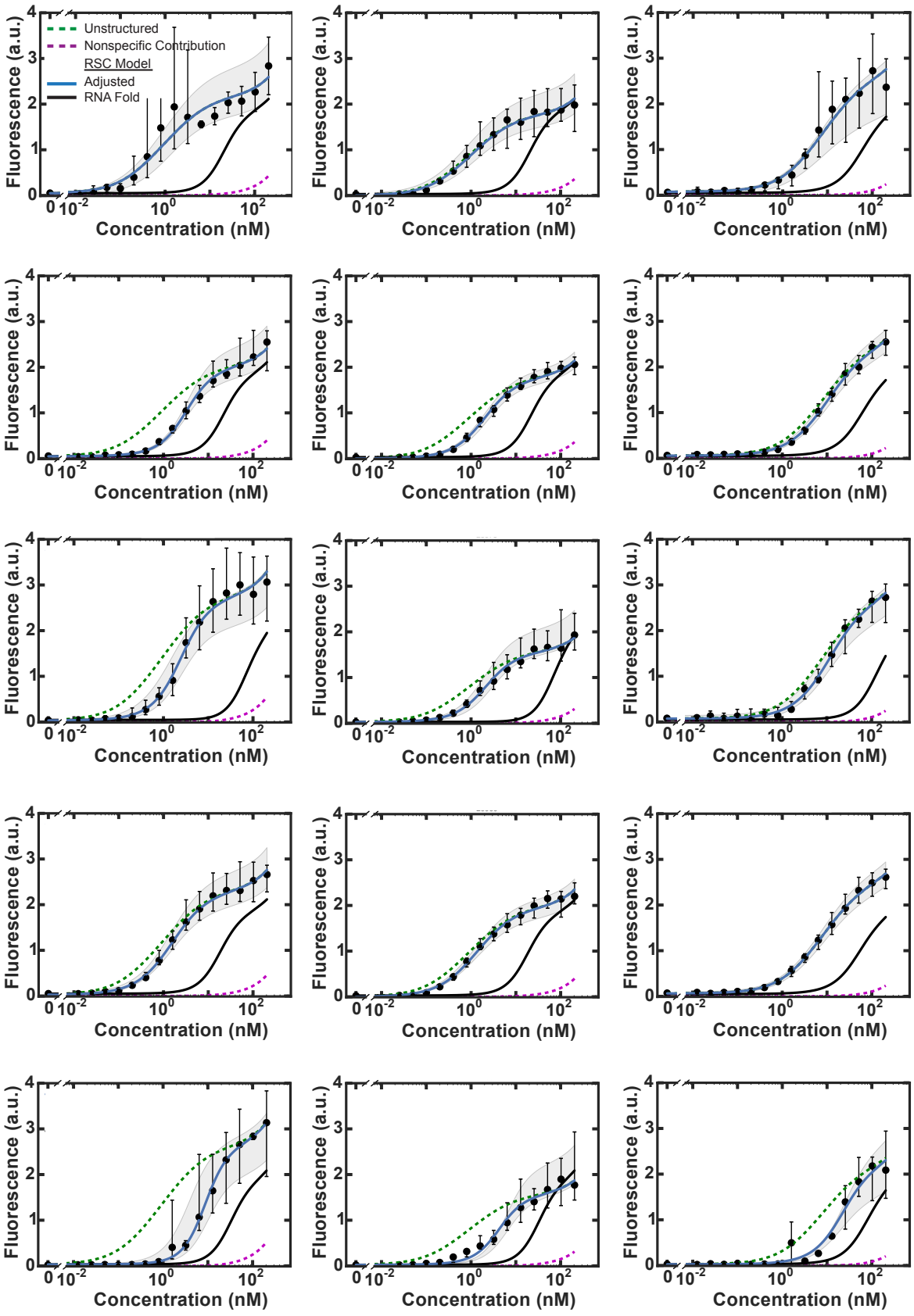
Unstructured
Nonspecific Contribution
RSC Model
Adjusted
RNA Fold
Fluorescence (a.u.)
Concentration (nM)
0
10^{-2}
10^{0}
10^{2}
0
1
2
3
4

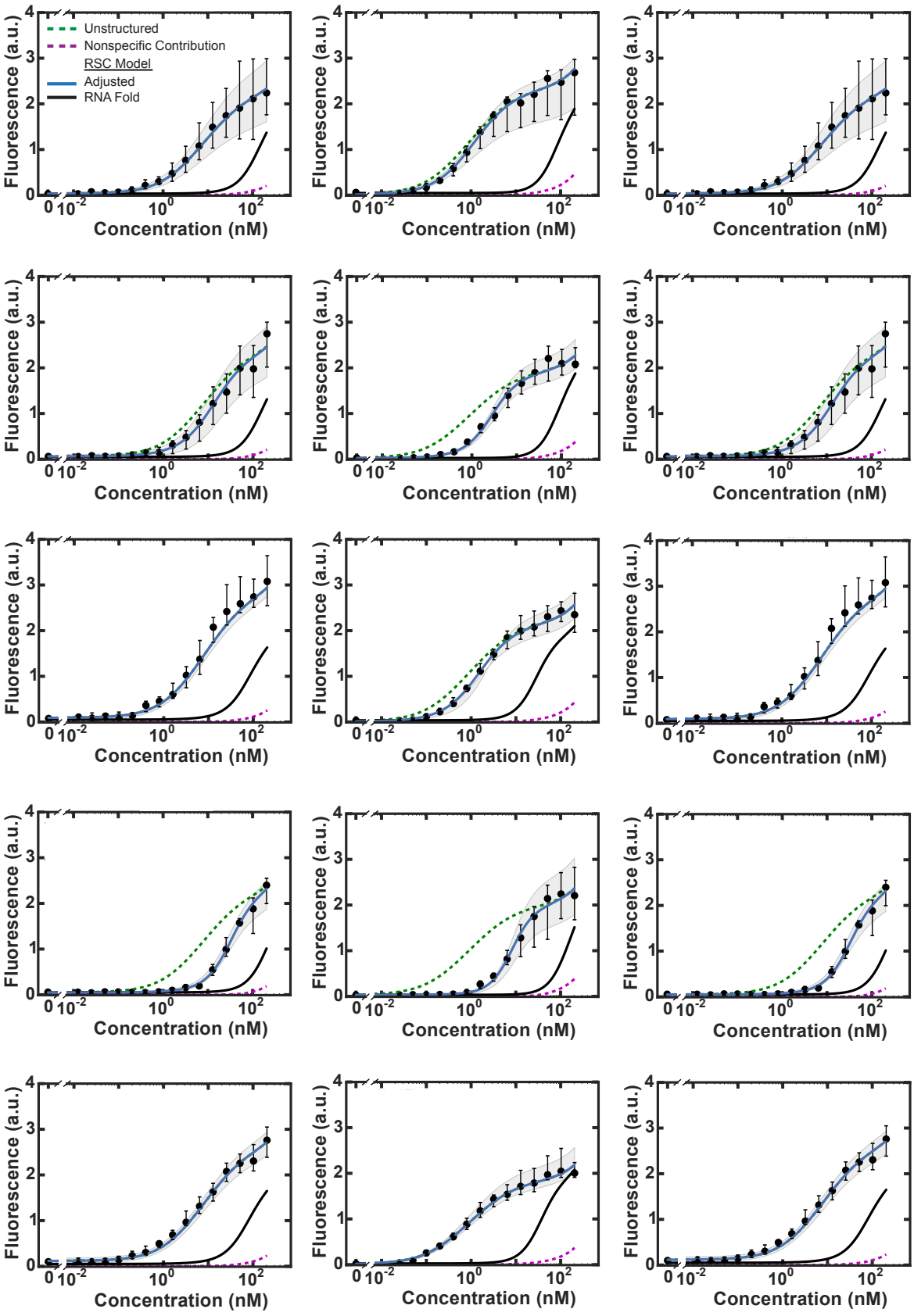
Unstructured
Nonspecific Contribution
RSC Model
Adjusted
RNA Fold
Fluorescence (a.u.)
Concentration (nM)
0
10^{-2}
10^{0}
10^{2}
0
1
2
3
4

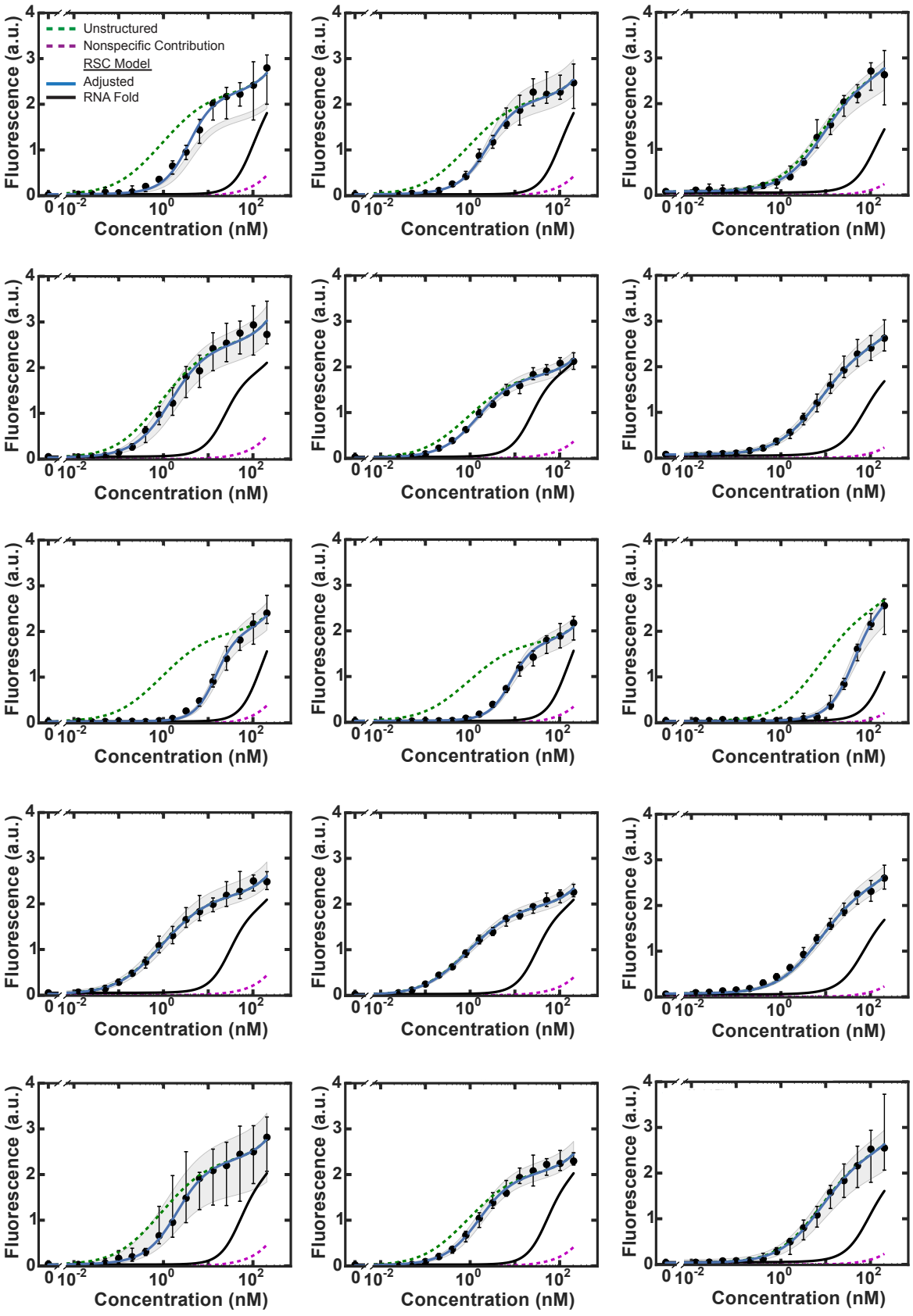
Unstructured
Nonspecific Contribution
RSC Model
Adjusted
RNA Fold
Fluorescence (a.u.)
Concentration (nM)
0
10^{-2}
10^{0}
10^{2}
0
1
2
3
4

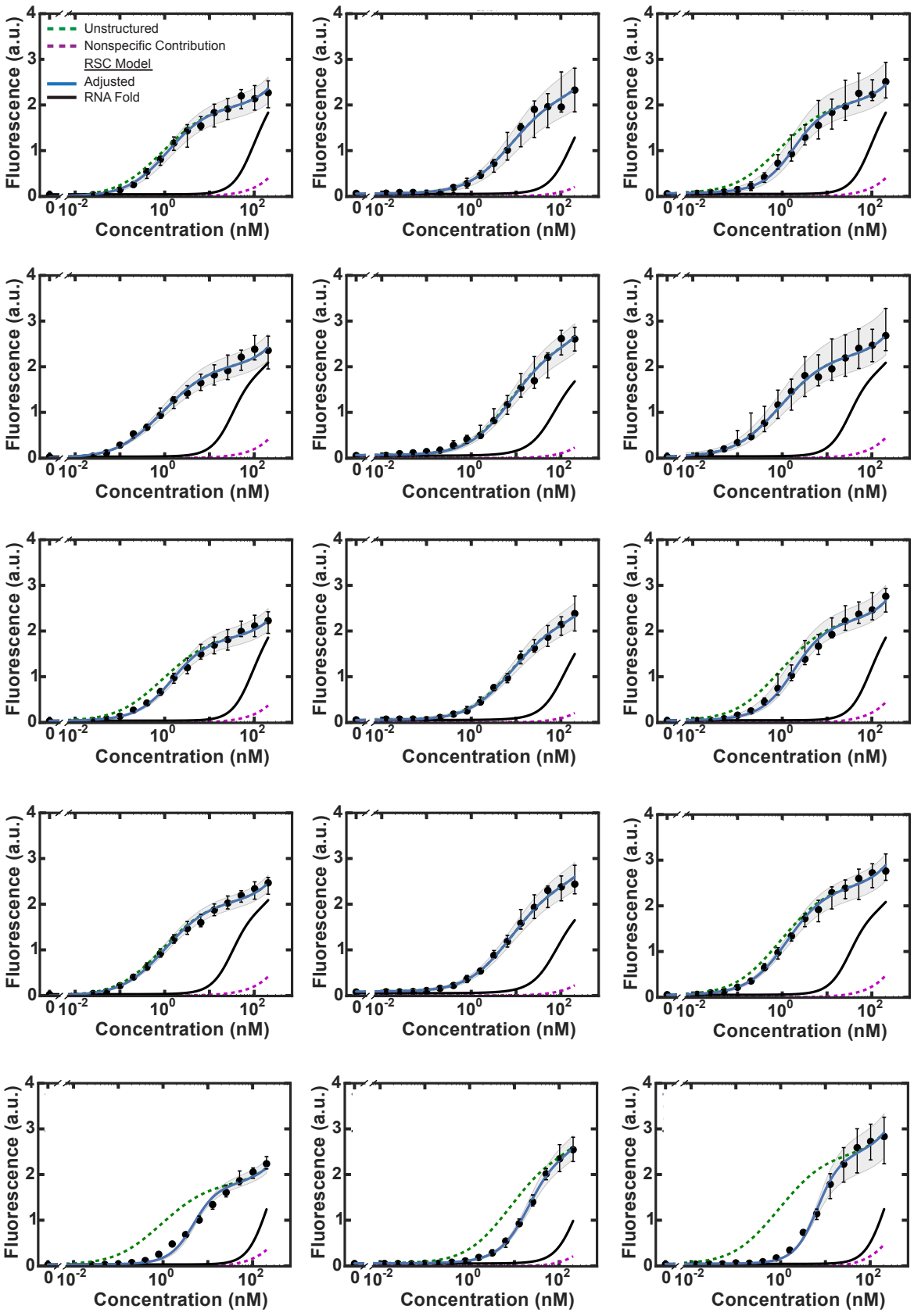
Unstructured
Nonspecific Contribution
RSC Model
Adjusted
RNA Fold
Fluorescence (a.u.)
Concentration (nM)
0
10^{-2}
10^{0}
10^{2}
0
1
2
3
4

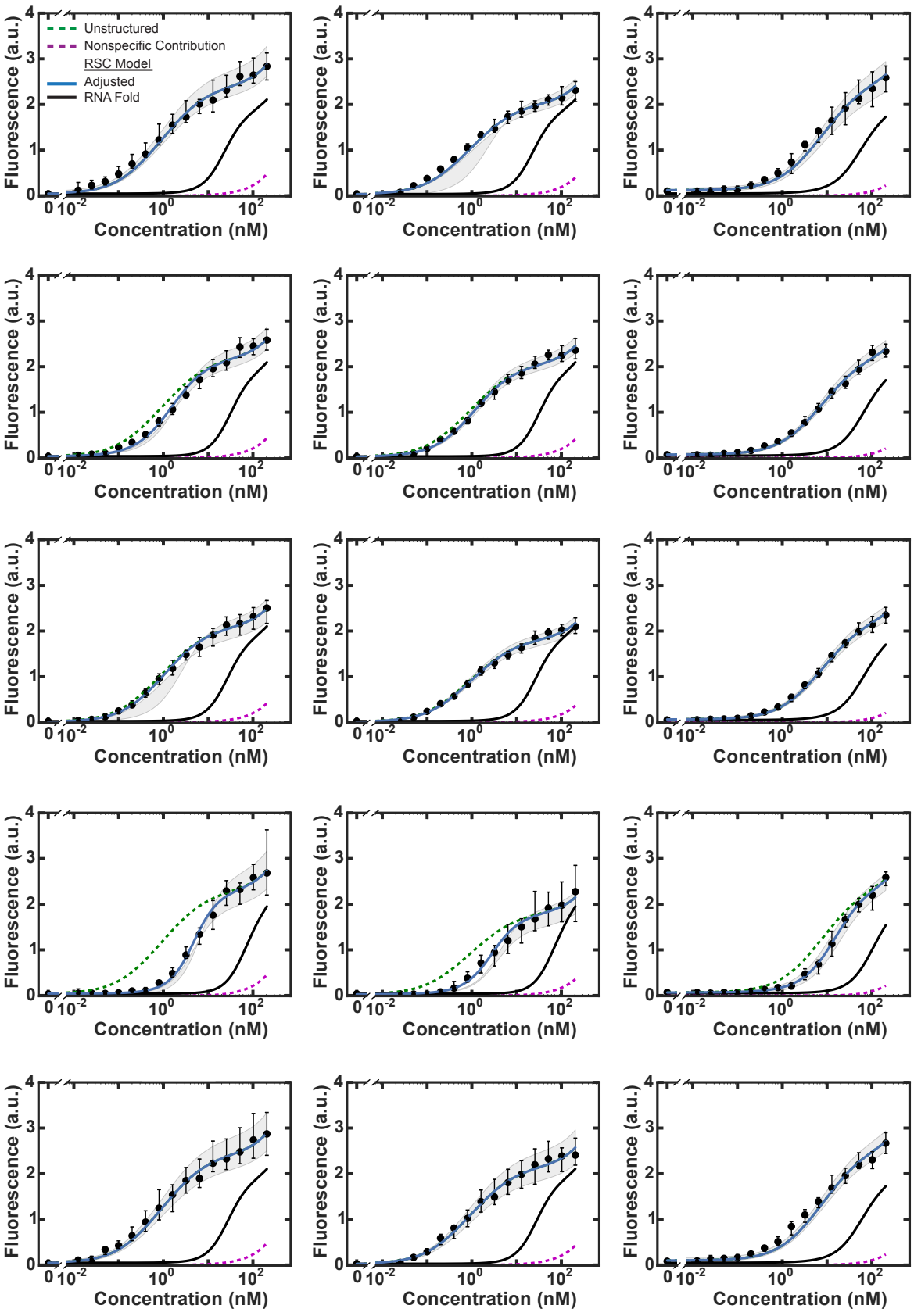
Unstructured
Nonspecific Contribution
RSC Model
Adjusted
RNA Fold
Fluorescence (a.u.)
Concentration (nM)
0
10^{-2}
10^{0}
10^{2}
0
1
2
3
4

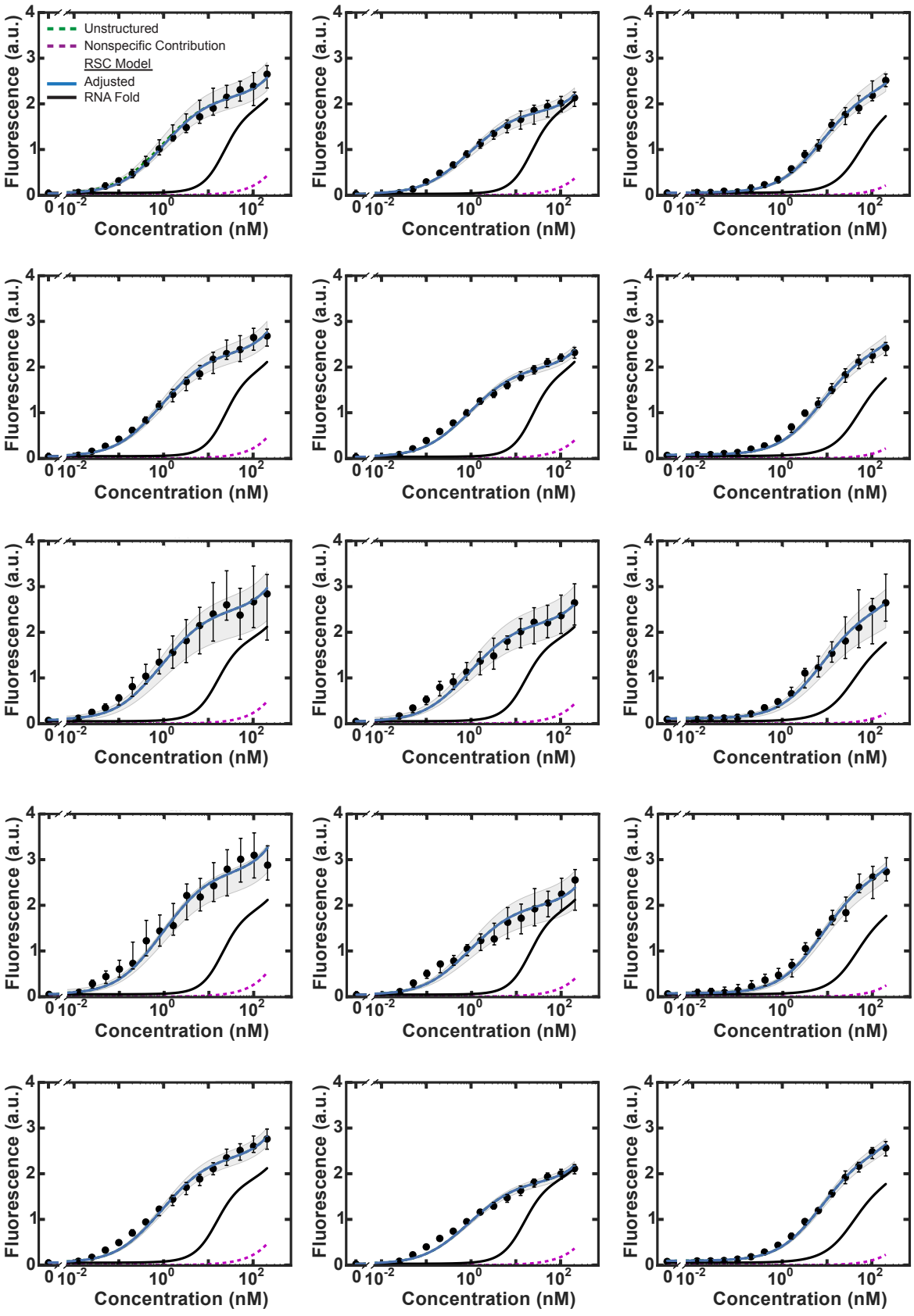
Unstructured
Nonspecific Contribution
RSC Model
Adjusted
RNA Fold
Fluorescence (a.u.)
Concentration (nM)
0
10^{-2}
10^{0}
10^{2}
1
2
3
4

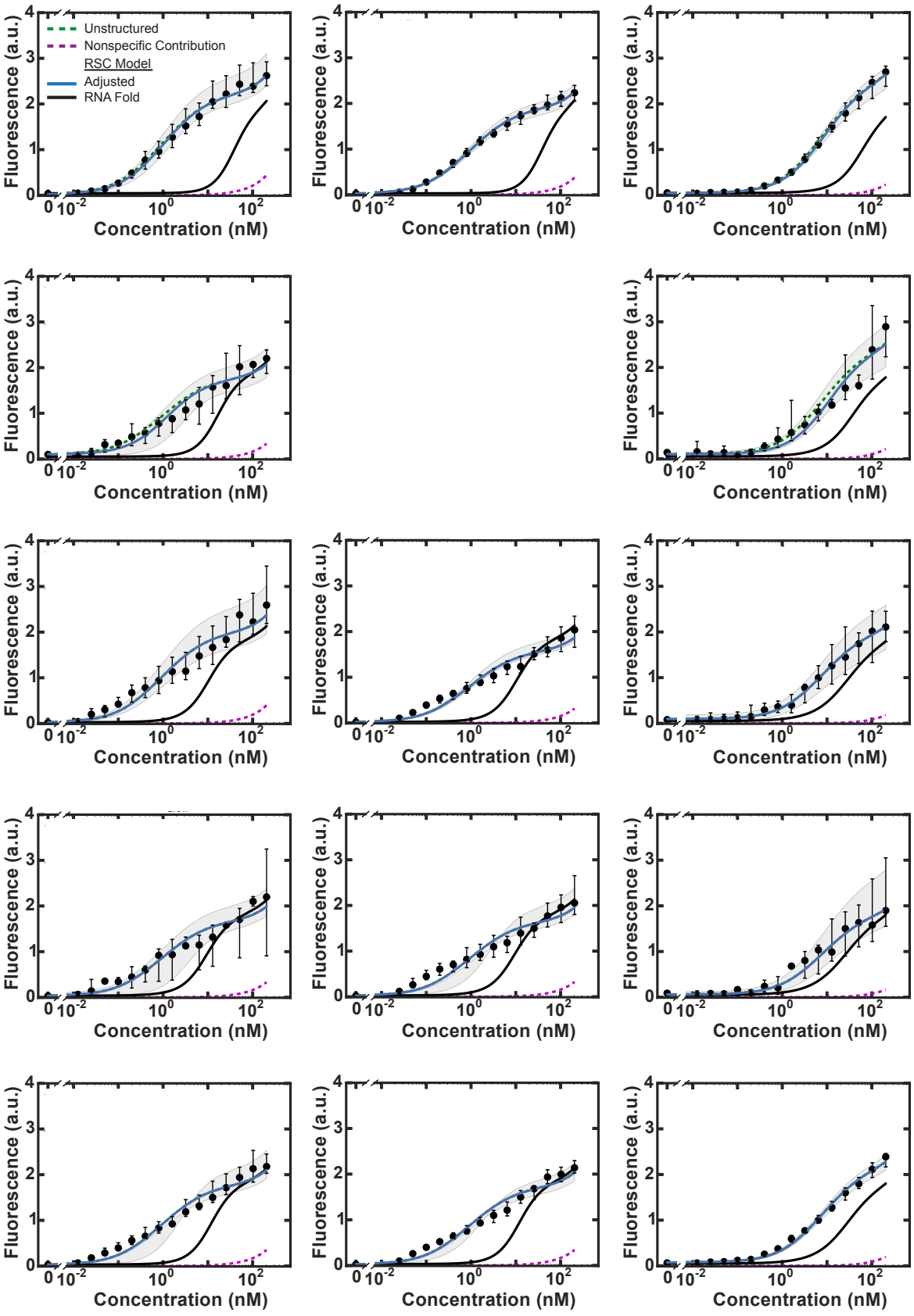
Unstructured
Nonspecific Contribution
RSC Model
Adjusted
RNA Fold
Fluorescence (a.u.)
Concentration (nM)
0
10^{-2}
10^{0}
10^{2}
1
2
3
4

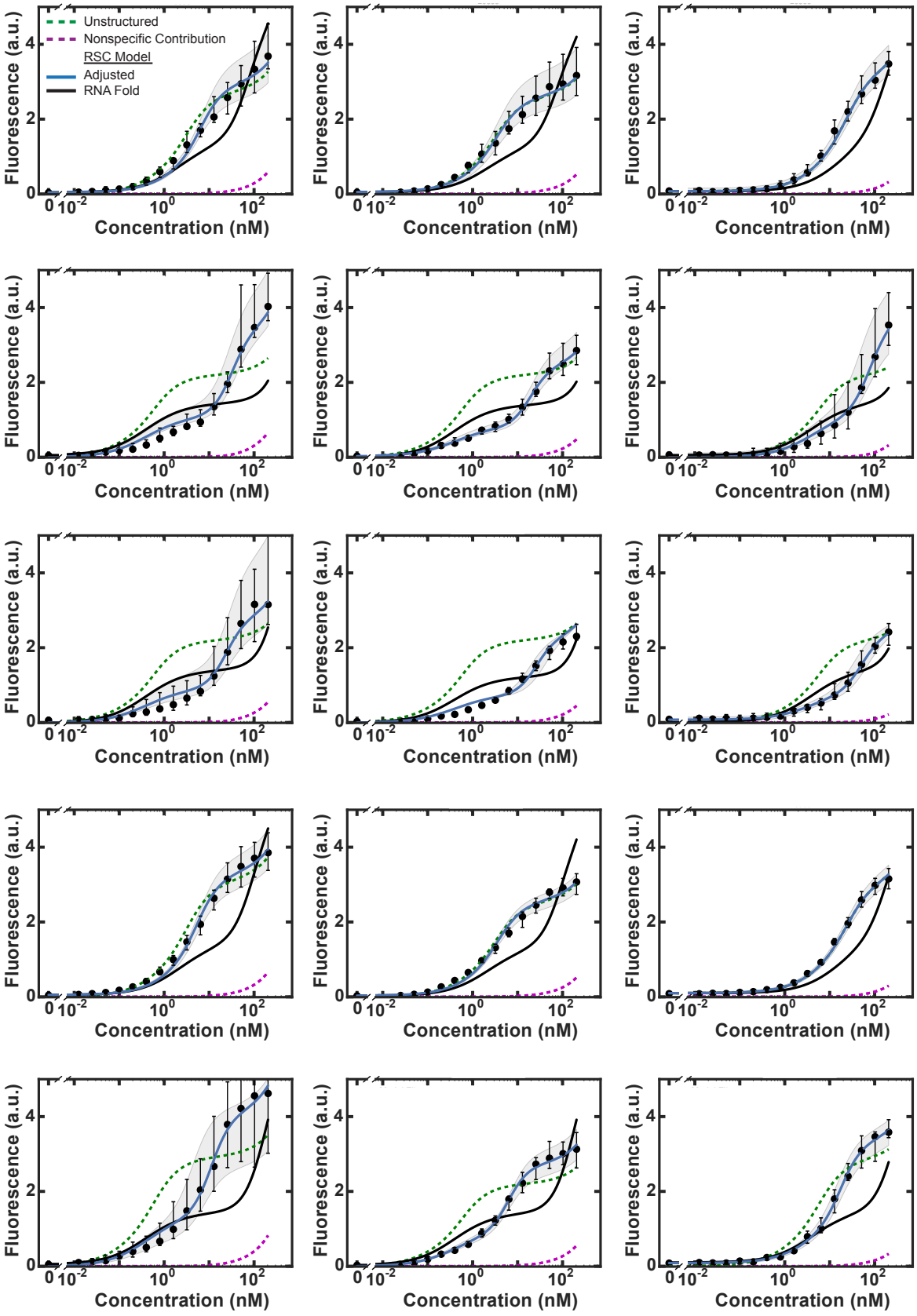
Unstructured
Nonspecific Contribution
RSC Model
Adjusted
RNA Fold
Fluorescence (a.u.)
Concentration (nM)
0
10^{-2}
10^{0}
10^{2}
0
2
4

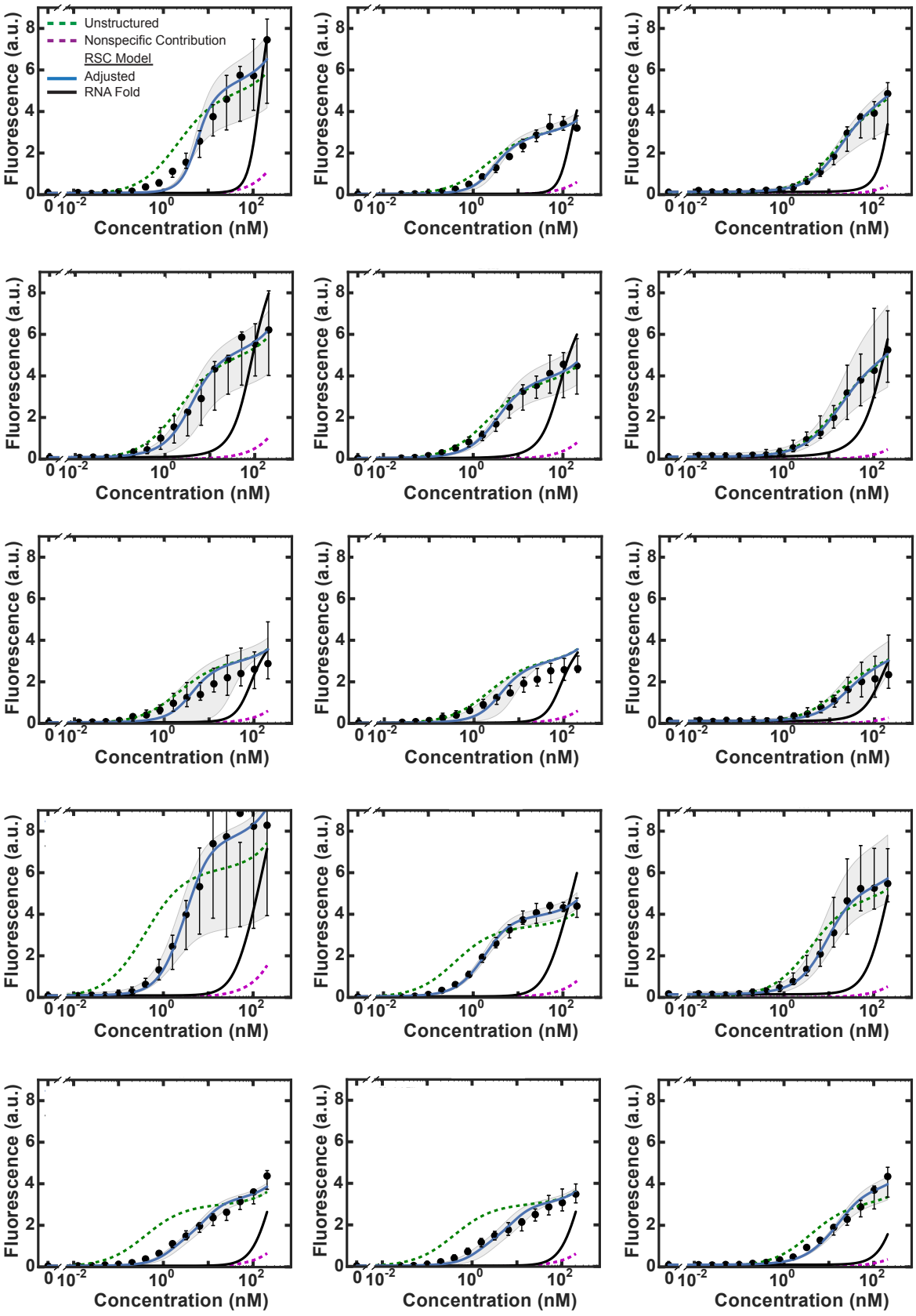
Unstructured
Nonspecific Contribution
RSC Model
Adjusted
RNA Fold
Fluorescence (a.u.)
Concentration (nM)
0
10^{-2}
10^{0}
10^{2}
0
2
4
6
8

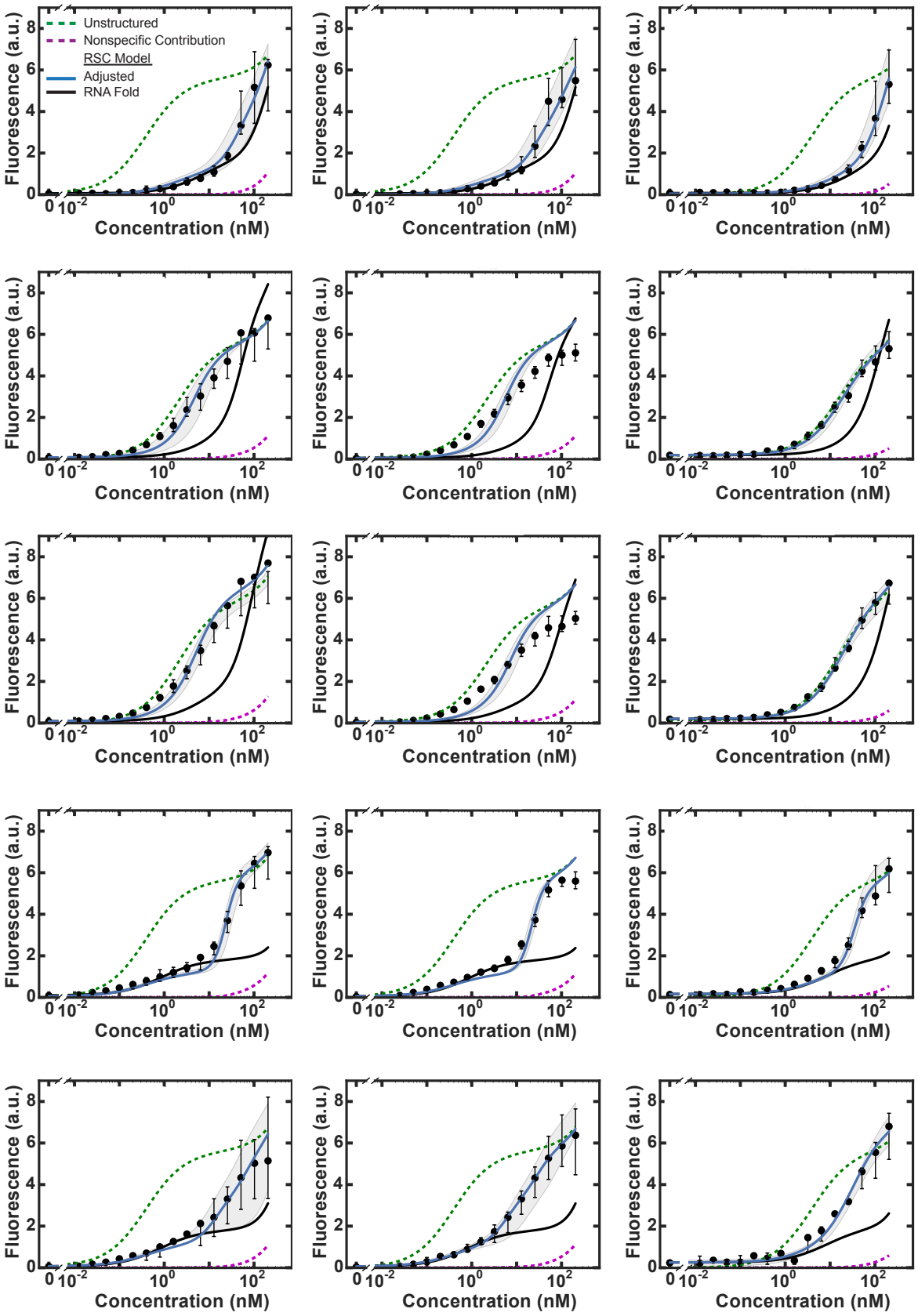
Unstructured
Nonspecific Contribution
RSC Model
Adjusted
RNA Fold
Fluorescence (a.u.)
Concentration (nM)
0
10^{-2}
10^{0}
10^{2}
0
2
4
6
8

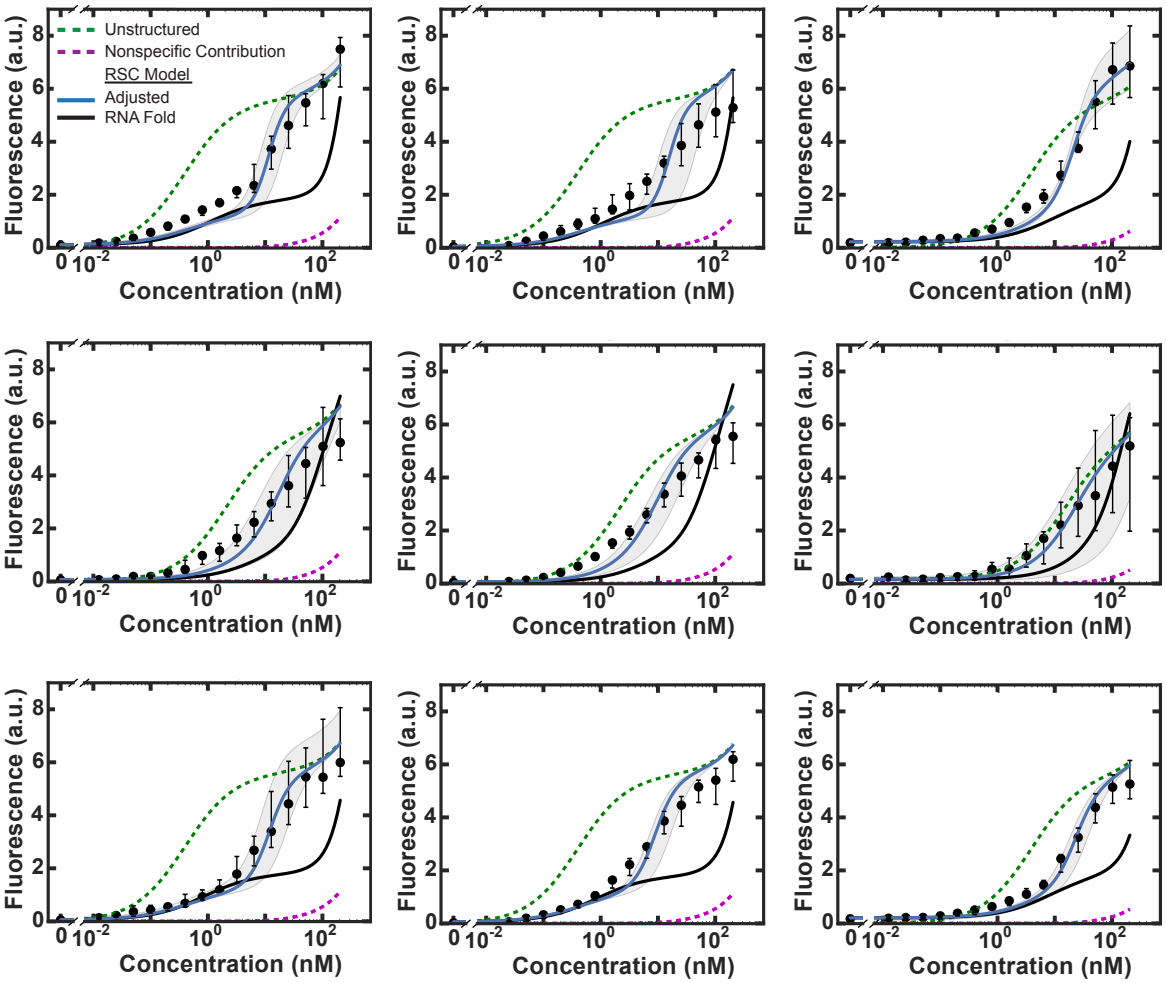

Figure S4: Binding curves for RNA constructs in this study at 25 °C (left and middle, independent replicates) and 37 °C (right).

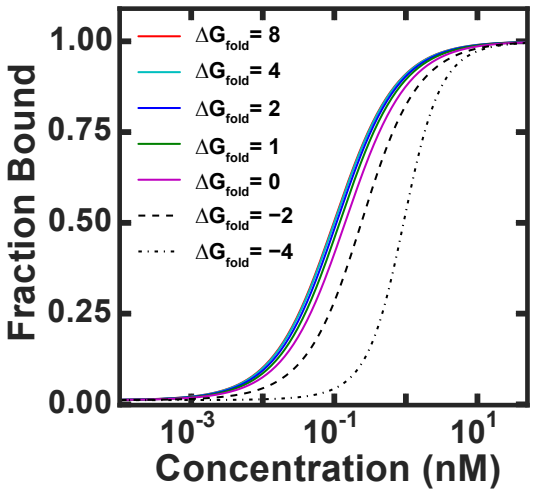

Figure S5: Binding curves for RNAs with two binding sites that form secondary structures with differential stabilities demonstrating that positive values of ΔG_{fold} (solid lines) have limited effects on the shape of the binding curve.

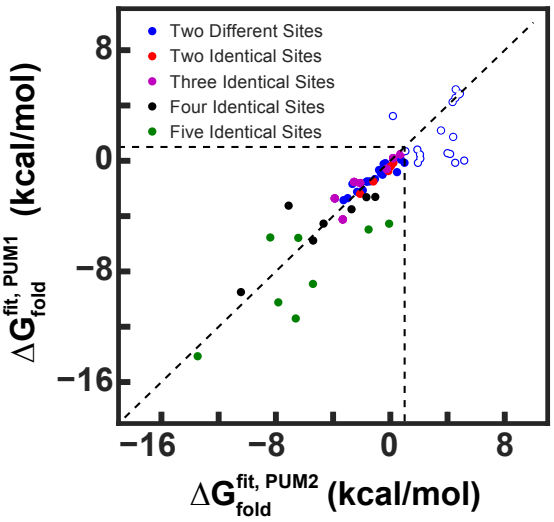

Figure S6: Relationship between ΔG_{fold} values computed for PUM1 and PUM2 binding.

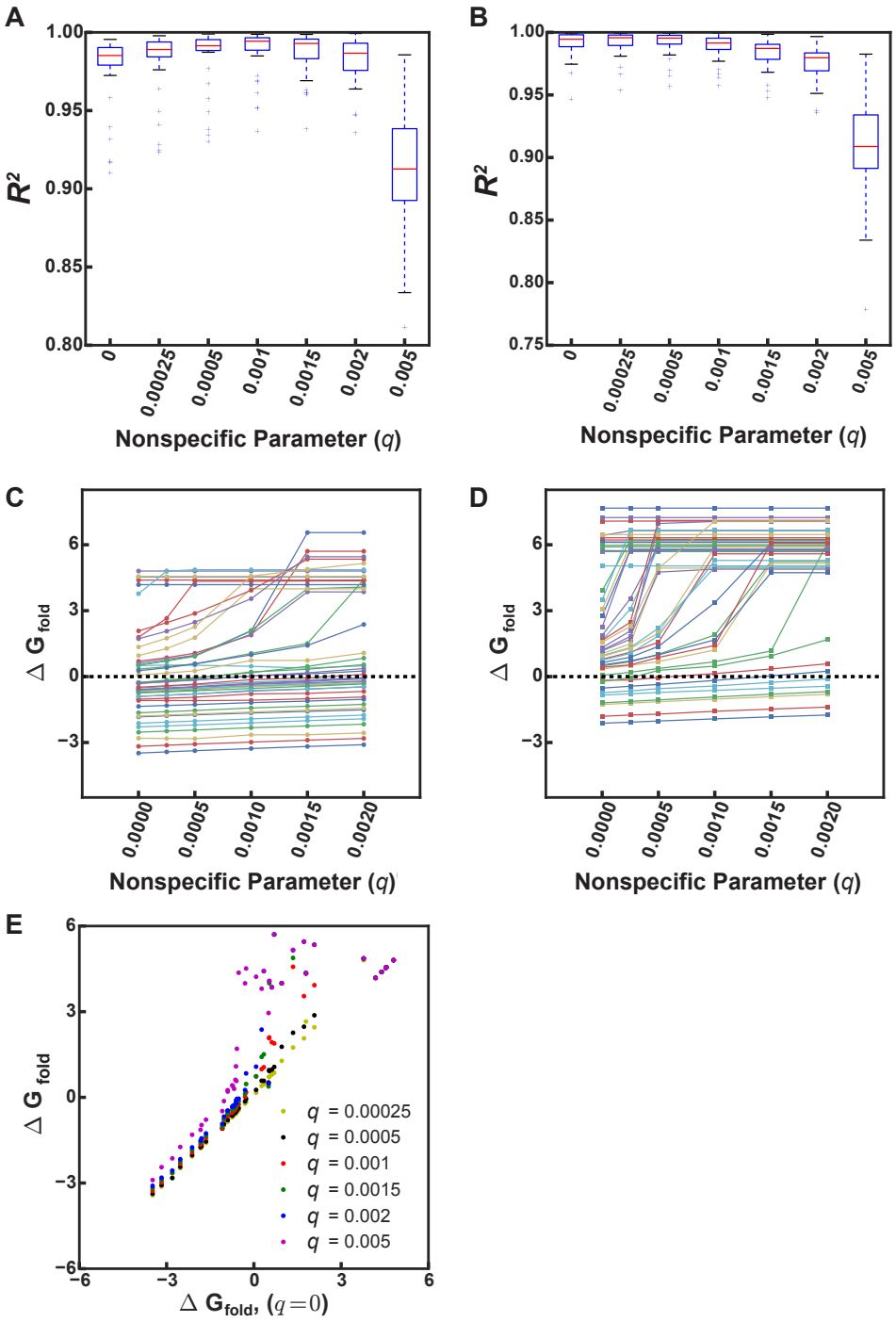

Figure S7: Determination of nonspecific term and sensitivity of fits to different nonspecific parameters. (A, B) R^2 values as a function of the constant value used for the nonspecific term for fitting 25 °C (A) and 37 °C (B) binding data. (C, D) Sensitivity of ΔG_{fold} values resulting from fitting the data with different values for the nonspecific parameter at 25 °C (C) and 37 °C (D). e) Relationship between ΔG_{fold} values obtained when fitting without the nonspecific term (x axis; q = 0) and when fitting with increasing values of the nonspecific term.